THE ASTROPHYSICAL JOURNAL, 239:859–866, 1980 August 1

FAR-ULTRAVIOLET STUDIES. VII. THE SPECTRUM AND LATITUDE DEPENDENCE OF THE LOCAL INTERSTELLAR RADIATION FIELD

R. C. HENRY, R. C. ANDERSON, AND W. G. FASTIE
Physics Department, Johns Hopkins University
Received 1979 October 22; accepted 1980 January 18

ABSTRACT

A direct measurement has been made of the spectrum (1180–1680 Å) and Gould-latitude dependence of the local interstellar radiation field, over about one-third of the sky. The result is corrected to give expected values for the entire sky. The average local 1180–1680 Å energy density is 5.8×10^{-17} ergs cm^{-3} Å^{-1}. The surface brightness falls off toward high latitudes much more steeply than published models predict.

Subject headings: ultraviolet: spectra

I. INTRODUCTION

The far-ultraviolet radiation field in interstellar space is of great interest because of its use in determining the rate of destruction of interstellar molecules. For example, Jura (1974) used a computed radiation field in a discussion of the formation and destruction of interstellar H_2.

The only available observational measurement of the far-UV interstellar radiation field is that of Henry *et al.* (1977, Paper II), who flew a photometer sensitive at 1530 Å on an Aerobee rocket. About half of the sky was scanned. In the present paper, we present the results of observing almost one-third of the sky with the far-UV spectrometer that was carried in the service module of the *Apollo 17* spacecraft (Fastie 1973).

The spectrometer scanned from 1180 Å to 1680 Å, with a resolution of 11 Å. During trans-Earth coast, many astronomical observations were made (Fig. 1). Targets marked "SPICA" and "α Eri" were observed for the purpose of absolute calibration of UV stellar brightnesses (Henry *et al.* 1975), while targets marked "III" include portions of the Large Magellanic Cloud (Henry, Feldman, and Fastie 1976; these observations were made from lunar orbit, from altitudes of 14 and 60 nautical miles. [Roman numerals I and II, not in the Fig., refer to nonastronomical observational modes in lunar orbit, while IV marks a search for zodiacal light.]) Targets marked "LY α MIN" and "NEP" were observed in a search for diffuse galactic light scattered at large angles (Henry *et al.* 1978, Paper III), while targets marked "DARK NORTH," "COMA," "VIRGO," and "DARK SOUTH" were observed in a successful search for diffuse radiation at high galactic latitudes (Henry *et al.* 1978, Paper IV).

During astronaut sleep periods, and on a number of other occasions, the spacecraft was placed in a "passive thermal control" (PTC), "rotisserie," mode, in which the spectrometer line of sight passed across large regions of the sky (large "small circles" in Fig. 1). The data acquired have been analyzed by Anderson, Henry, and Fastie (1980, Paper VI), in a search for large-scattering angle diffuse galactic light; those authors provide details regarding the individual scans. In the present paper we discuss the raw observed flux, to determine the nature of the local interstellar radiation field.

II. THE DATA

An example of the data that were obtained is given in Figure 2, where the observed intensity in the wavelength region 1385 to 1474 Å is plotted against time (*solid line*, *lower panel*), for the first hour or so of the second sleep PTC period. Grating-scattered Lα radiation has been removed (see Paper VI). The dashed line in the lower panel gives the expected brightness that is obtained by integrating the SAO star catalog (Whipple 1966), calibrated to the far-UV (Henry 1977, Paper I). The upper panel gives the observed solar-system Lα intensity as a function of time and the average 21 cm column density in the spectrometer line of sight from Heiles (1975).

The brightnesses in Figure 2 are linear below the horizontal line and logarithmic above it. A rather different impression of the data is given in Figure 3, which shows the brightness observed during the first hour of the first sleep PTC period, on a linear scale, for a variety of wavelength intervals. A striking feature is the observation of the planet Earth, about 16 minutes into the scan. The observations of Earth were deleted from the data set for the purposes of the present paper.

III. DATA ANALYSIS

The spectrometer field of view was 12° × 12°. Since the pointing direction of the spectrometer changed significantly (~3°) during the obtaining of each 12 s spectrum, individual pointing positions were computed for the mid-time of each of six wavelength regions. For these positions and wavelengths, the

1980ApJ...239..859H

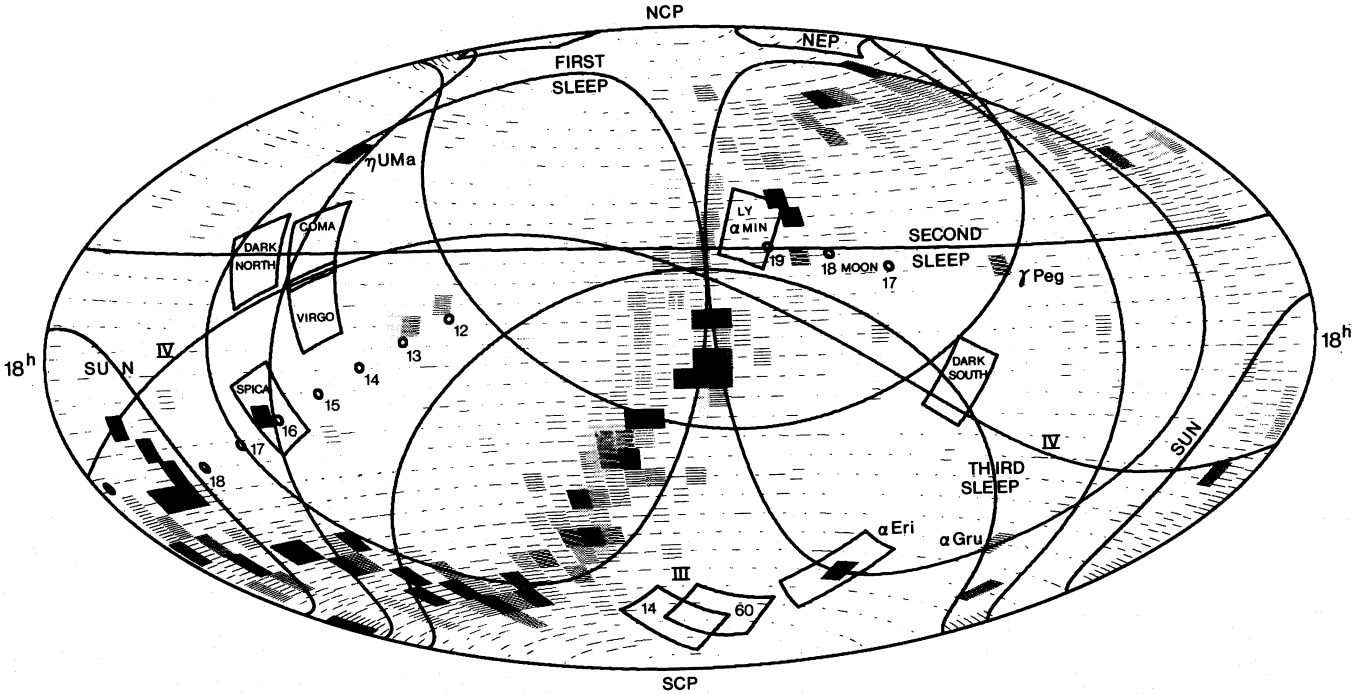

FIG. 1.—An Aitoff equal-area map of the sky, in celestial coordinates, with 18 hr at the edge of the map and north at the top. Shading represents the far-UV surface brightness of the sky at 1470 Å that is expected according to the star catalog integration of Henry 1977 (Paper I). A "circle of avoidance" of radius 30° is drawn around the position of the Sun. Positions of the Moon (as observed from Earth) and of the Earth (as observed from the Moon) are given for a number of dates in 1972 December. Several astronomical targets are marked; these are described in the text. The data discussed in the present paper were obtained during large-scale sky scans, including scans made during the 3 astronaut sleep periods.

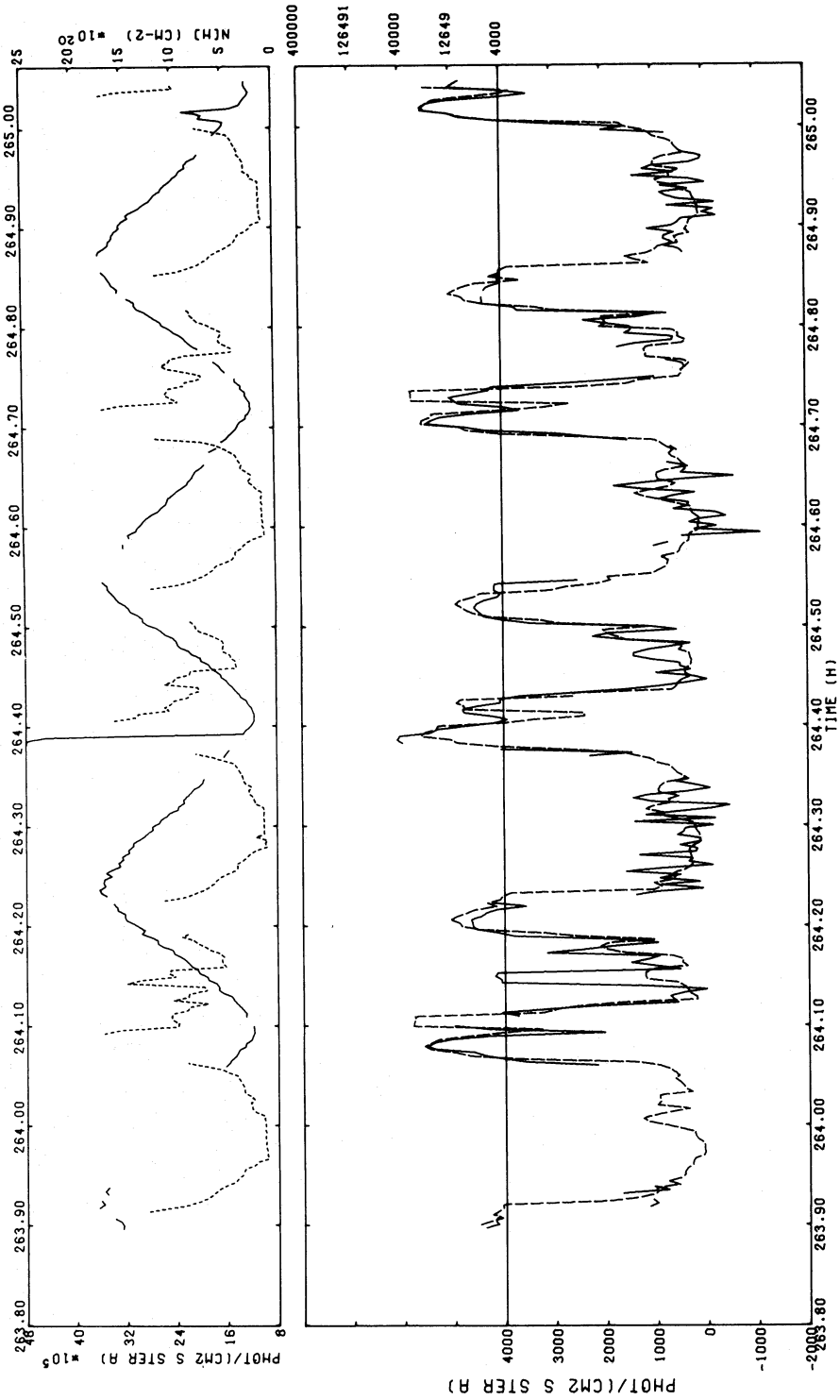

FIG. 2.—The observed brightness of the sky in the wavelength range 1385–1474 Å is plotted (*solid line in lower panel*) against time, for the first hour of the second sleep PTC period. The scale is linear below the horizontal line and logarithmic above it. Grating-scattered Lα radiation has been removed. The dashed line in the lower panel represents the expected signal, from integration of the expected brightness of SAO catalog stars in the field of view. In the upper panel, the solid line represents the observed intensity of solar system Lα radiation (the sharp spike represents observation of the Moon), while the dashed line gives the 21 cm column density in the field of view, from Heiles (1975).

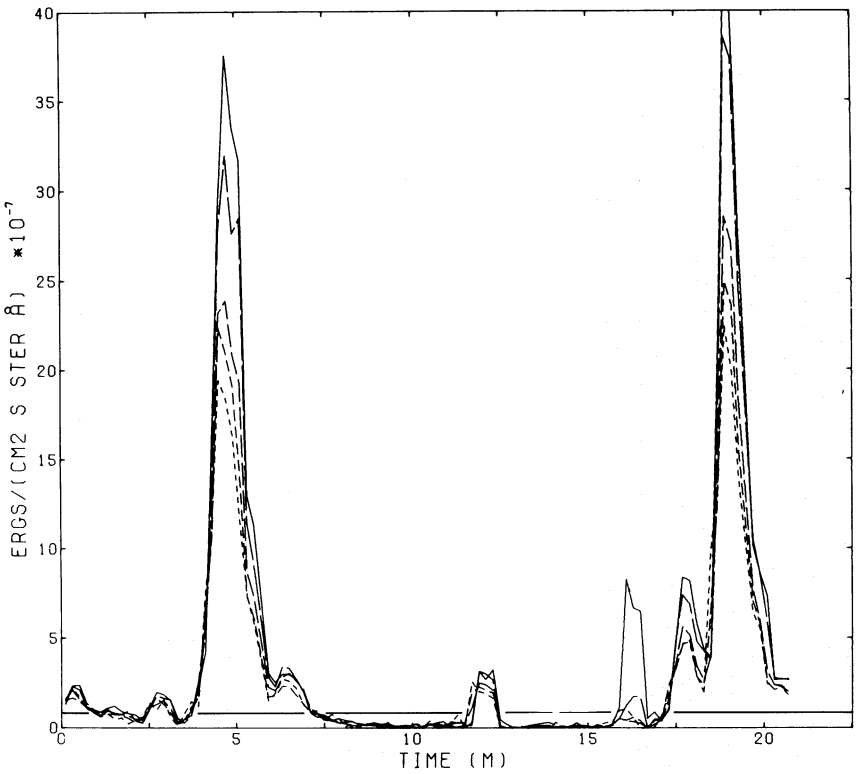

FIG. 3.—The observed brightness, as a function of time, for the first spacecraft rotation during sleep PTC period 1, for the wavelength intervals 1246–1313 Å (*solid line*), 1313–1385 Å (*long dashes*), 1385–1473 Å (*shorter dashes*), 1473–1558 Å (*still shorter dashes*), and 1558–1669 Å (*shortest dashes*). The intensity scale is linear. The planet Earth, observed about 16 minutes into the scan, is bright at 1304 Å (O I emission). The horizontal lines are used to divide the sky into "bright" (*above the line*) and "dim" (*below the line*) regions (see Fig. 5).

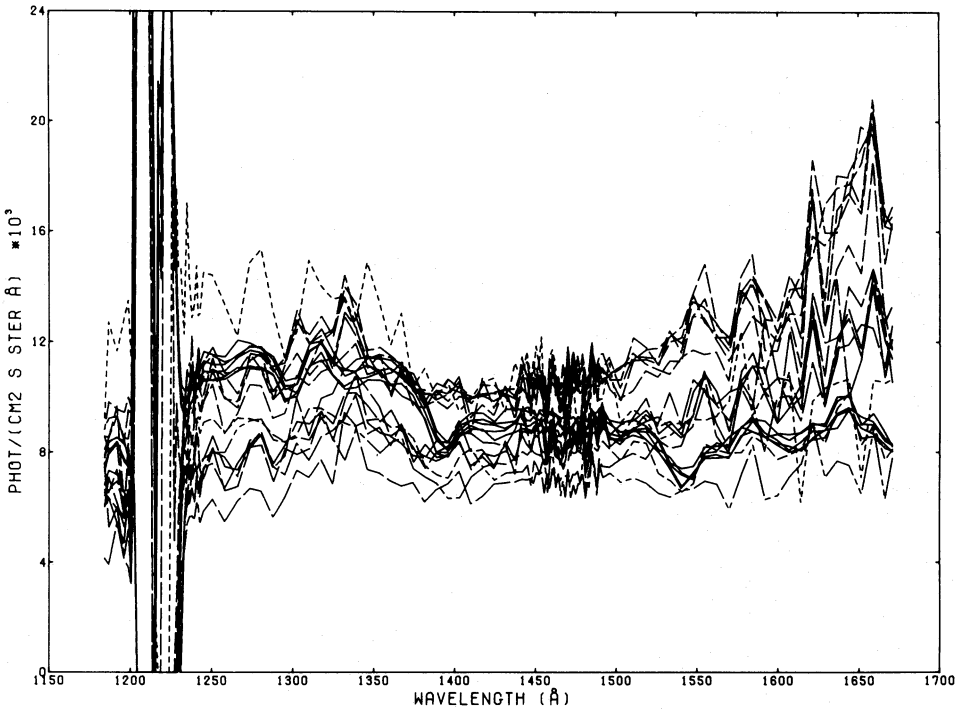

FIG. 4.—The average surface brightness of the sky was obtained by averaging all of the data, in approximately 2 hr segments, after normalizing each observation using a star catalog integration as an intermediary. A variety of plotting symbols are used to guide the eye, but the main purpose of the Fig. is to convey an impression of the scatter in the processed data. This scatter results essentially entirely from the 1° uncertainty in the line of sight of the spectrometer at any given time.

calibration of Paper I was used to convert from the magnitude and spectral class of the SAO catalog, to intensity units, for each early-type (OBAF) star in the field of view; the result was summed over all of the stars in the field of view. The spectrum of the interstellar radiation field can be obtained from a single spectrometer scan by using this star catalog integration as an intermediary. The observed spectrum is simply divided by the ratio of the star catalog integration (interpolating in wavelength where necessary) for that target to the star catalog integration for the whole sky. Many of the deficiencies of the star catalog integration will cancel out in this process, but certain others (such as the fact that interstellar absorption is not explicitly allowed for) will remain. A better result will be obtained by averaging the radiation field that is deduced from large numbers of spectra obtained during observation of many different regions on the sky. To the extent that a *representative* selection of sky regions is observed, the star catalog integration will cancel out entirely. The scan paths shown in Figure 1 indicate that a resonably representative one-third of the sky was actually observed.

In Figure 4 we show the result of averaging the radiation fields deduced from scans of each of PTCs 4, 5, and 6 and also averaging the radiation fields obtained using many 2 hr segments of the longer PTCs 1, 2, and 3 (see Paper VI for details of the various PTC scans). We do not attempt to identify the deduced radiation fields individually (although they are coded, to some extent, to allow separate sections of the same spectrum to be identified); the purpose of the figure is to convey a visual impression of the scatter in the data. This scatter occurs largely because of the 1° absolute spacecraft pointing error. In Paper VI, where we were looking for a faint diffuse flux at moderate galactic latitudes, we computed an expected error due to pointing uncertainty and weighted spectra according to this error. That procedure tends to discount spectra from bright regions of the sky, which must be included for the present purpose. Instead, we allow for the effects of pointing error simply by averaging large numbers of spectra.

A powerful additional feeling for the uncertainties of the procedures may be gained by dividing the sky into "bright" and "dim" regions (the division is indicated in Fig. 3) and deducing the average whole sky brightness (radiation field) independently from each. The result of doing this is shown in Figure 5 for the three long-sleep PTCs. Solid lines show the result for dim regions, while dashed lines give the result for bright regions. A systematic difference does appear, which is perhaps not surprising in view of the very large difference in brightness between dim and bright regions. Which is closer to the truth? It is not possible to tell. The error in the ratio of the star catalog integration of a bright region, to the integration for the whole sky, could result in just as much error as the error in the same ratio for a dim region. The sources of possible error (such as the failure to allow explicitly for

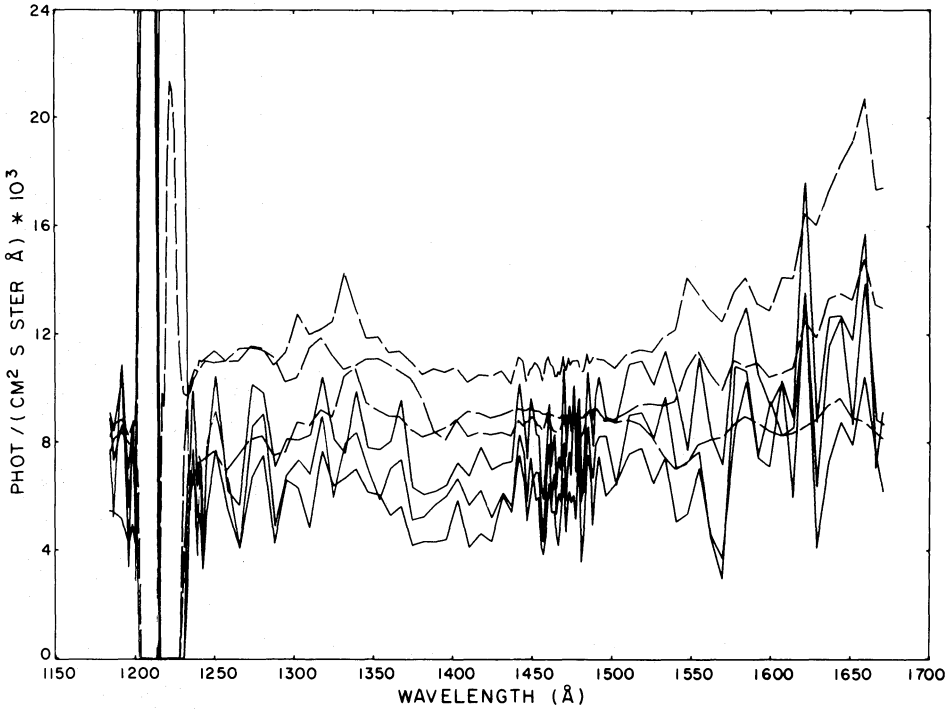

FIG. 5.—The average surface brightness of the sky as estimated separately from observation of bright regions (*dashed lines*) and dim regions (*solid lines*) of the sky (the regions are defined in Fig. 3), averaged over each of the three longest PTC observation periods. A systematic difference does appear, but it is not large, especially considering the very large difference in brightness between the bright and dim regions.

interstellar absorption) are many and are not susceptible to quantification; but the very reasonable result, given in Figure 5, that is obtained for a *very extreme* subdivision of the data, gives considerable confidence that systematic errors are not large. Also, we reiterate that, to the extent that we have in sum observed a *representative* selection of bright and dark regions, the star catalog integration will cancel out completely.

IV. RESULTS

In Figure 6 is shown (*solid histogram*) the final deduced average surface brightness of the entire sky. Each PTC has been given equal weight, regardless of the length of observation, because the longer PTCs simply involve repeated observation of essentially the same region of sky, so systematic errors will tend to repeat. The error bars represent the rms error in the mean of the six measurements. (No result could be obtained for the wavelength region near Lα because of the large solar-system Lα signal.) The radiation-field spectrum is given in Table 1. For comparison, Figure 6 includes the spectrum of the B5 IV star α Eri, observed with the same instrument (Henry *et al.* 1975) and the interstellar radiation field (*solid dots*) predicted in Paper I from a simple integration of the calibrated SAO star catalog.

It is also of interest to examine the latitude dependence of the interstellar far-UV radiation field. In Figure 7, we plot the observed 1385–1474 Å intensity (*solid line*) versus Gould latitude and compare this with the SAO star catalog integration for the same portion of the sky. The errors on the observational histogram are the rms errors corresponding to the scatter among the six PTCs, while the errors on the star catalog integration are simply the ±20% uncertainty that we have always claimed for this method (Paper I). Agreement is excellent.

The Gould-latitude dependence for the entire sky can be obtained by multiplying the latitude dependence measured for the part of the sky we observed by the ratio of the star-catalog integration over the entire sky (for the Gould-latitude dependence of the ra-

TABLE 1

FAR-ULTRAVIOLET INTERSTELLAR RADIATION FIELD

Wavelength (Å)	Ph $(cm^2\ s\ sr\ Å)^{-1}$	$\times 10^{-17}$ ergs $cm^{-3}\ Å^{-1}$
1195	7600	5.29
1250	9700	6.46
1300	10200	6.53
1350	10400	6.41
1400	8900	5.29
1450	9400	5.40
1500	9400	5.22
1550	9800	5.26
1600	10400	5.41
1650	12400	6.26

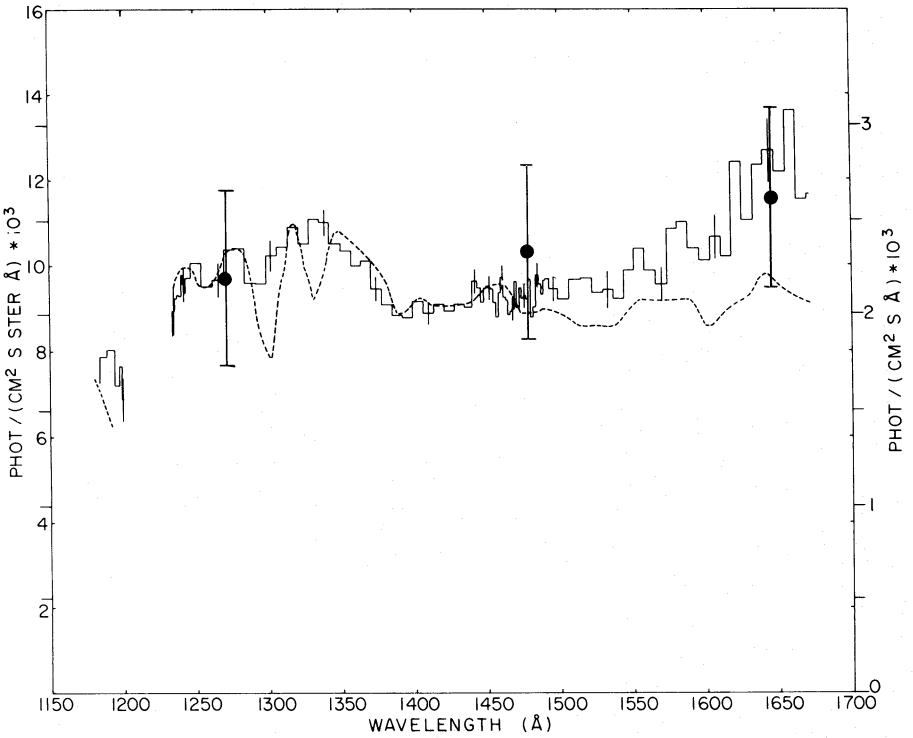

FIG. 6.—The spectrum of the local far-UV interstellar radiation field. This is the average surface brightness of the entire sky as estimated by combining the determinations from the six PTCs. The error bar is the error in the mean determined from the rms scatter among the 6 independent determinations. Solid dots represent the prediction of Paper I using the SAO star catalog; error bars represent the ±20% uncertainty claimed in that paper. The dashed line (right scale) gives, for comparison, the spectrum of the B5 IV star α Eri, observed with the same instrument.

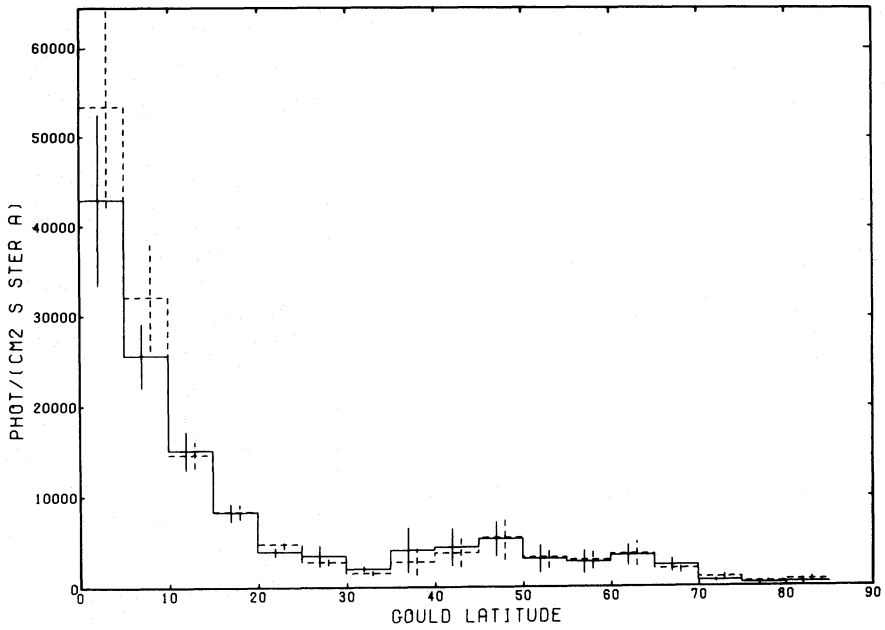

FIG. 7.—The observed (*solid line*) Gould-latitude dependence of the observed radiation (1385–1474 Å) is compared with the prediction of the star-catalog integration (*dashed line*) for the same part of the sky. Agreement is excellent. Errors in the data are rms errors; errors attached to the star-catalog histogram are ±20% estimated uncertainties from Paper I. Note that this Fig. refers to only a part of the sky; the result corrected to the whole sky is given in Fig. 8.

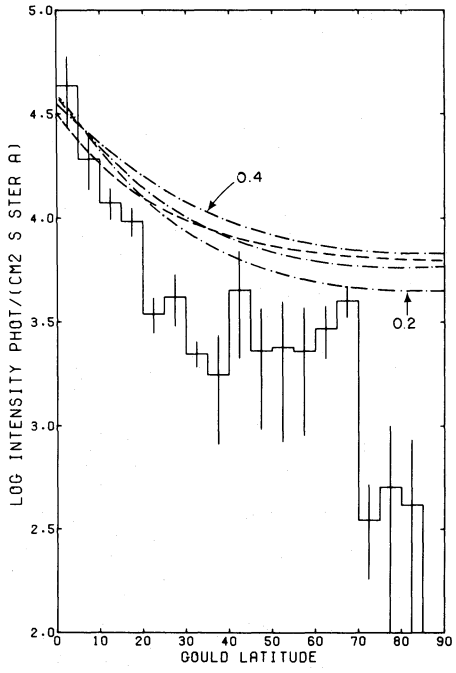

FIG. 8.—"Observed" (i.e., using the star-catalog integration only as an *intermediary*) Gould-latitude dependence of the interstellar far-UV radiation (1385–1474 Å) for the entire sky (*solid histogram*) is compared with the model of Gondhalekar and Wilson 1975 (*dashed line*). The observed "bump" at 40° to 70° is caused by a small number of rather bright stars. The dash-dotted lines represent the normalized "direct starlight" contribution to the models of van de Hulst and de Jong 1969 for three values (0.2, 0.3, 0.4) of the assumed optical thickness of the galaxy.

diation) with the same integration (Fig. 7) for the part of the sky we observed. The result (again for 1385–1474 Å) is compared in Figure 8 with the galactic-latitude dependence of the interstellar far-UV radiation field of Gondhalekar and Wilson (1975), and the "direct starlight" contribution to the models of van de Hulst and de Jong (1969), for three values (0.2, 0.3, 0.4) of the assumed optical thickness of the galaxy (*dash-dotted lines*, normalized to the data and to each other at 5° latitude). The van de Hulst and de Jong (1969) models were computed with visible radiation in mind. The scales and proportions of the figure are identical to those of Figure 5 of Paper II, to allow comparison with the observed galactic-latitude dependence reported there; agreement is excellent, except at the very highest latitudes, where we now find a very much lower surface brightness. The high surface brightness at the pole found in Paper II was attributed to residual airglow; the present observations were made about halfway between the Earth and the Moon.

V. CONCLUSION

The spectrum of the local far-UV radiation field has been measured between 1180 and 1680 Å (Fig. 6; Table 1). The intensity, spectrum, and latitude dependence are very well predicted by the SAO star-catalog integrations of Paper I. The sky brightness falls off much more steeply with Gould latitude (Fig. 8)

than models predict. These results apply, of course, to our own particular spot in the galactic plane; the radiation field undoubtedly will be substantially different at other locations in the spiral arms.

We thank our colleagues on *Apollo 17*. This work was supported by NASA contract NAS 9-11528 and NASA grant NGR 21-001-001 to the Johns Hopkins University.

REFERENCES

Anderson, R. C., Henry, R. C., and Fastie, W. G. 1980, *Ap. J.*, submitted (Paper VI).
Fastie, W. G. 1973, *Moon*, **7**, 49.
Gondhalekar, P. M., and Wilson, R. 1975, *Astr. Ap.*, **38**, 329.
Heiles, C. 1975, *Astr. Ap. Suppl.*, **20**, 37.
Henry, R. C. 1977, *Ap. J. Suppl.*, **33**, 451 (Paper I).
Henry, R. C., Anderson, R., Feldman, P. D., and Fastie, W. G. 1978, *Ap. J.*, **222**, 902 (Paper III).
Henry, R. C., Feldman, P. D., and Fastie, W. G. 1976, *Astr. Ap.*, **53**, 317.
Henry, R. C., Feldman, P. D., Fastie, W. G., and Weinstein, A. 1978, *Ap. J.*, **223**, 437 (Paper IV).
Henry, R. C., Swandic, J. R., Shulman, S. D., and Fritz, G. 1977, *Ap. J.*, **212**, 707 (Paper II).
Henry, R. C., Weinstein, A., Feldman, P. D., Fastie, W. G., and Moos, H. W. 1975, *Ap. J.*, **201**, 613.
Jura, M. 1974, *Ap. J.*, **191**, 375.
van de Hulst, H. C., and de Jong, T. 1969, *Physica*, **41**, 151.
Whipple, F. L. 1966, *Smithsonian Astrophysical Observatory Star Catalog* (Washington: Smithsonian Institution Press).

R. C. Anderson: Hughes Aircraft Company, Centilela and Teale Streets, Building 6 C-143, Culver City, CA 90230

W. G. Fastie and R. C. Henry: Physics Department, Johns Hopkins University, Baltimore, MD 21218